# Role of Peptide Structure in Lipid–Peptide Interactions: High-Sensitivity Differential Scanning Calorimetry and Electron Spin Resonance Studies of the Structural Properties of Dimyristoylphosphatidylcholine Membranes Interacting with Pentagastrin-Related Pentapeptides†

Witold K. Surewicz‡ and Richard M. Epand*

*Department of Biochemistry, McMaster University, Health Sciences Centre, Hamilton, Ontario L8N 3Z5, Canada*

*Received October 1, 1984*

ABSTRACT: The effects of amino acid substitutions in the pentapeptide pentagastrin on the nature of its interactions with dimyristoylphosphatidylcholine (DMPC) are assessed by differential scanning calorimetry and electron spin resonance. In two peptide analogues, the Asp at position 4 in pentagastrin (*N*-*t*-Boc-β-Ala-Trp-Met-Asp-Phe-$NH_2$) is replaced by Gly or Phe. These uncharged, more hydrophobic peptides have little effect on the transition temperature of DMPC, but they broaden the transition and lower the transition enthalpy as do integral membrane proteins. These peptides also mimic the behavior of integral membrane proteins in decreasing the order of a 5-doxylstearic acid spin probe below the transition temperature and in exhibiting a second immobilized lipid component using a 16-doxylstearic acid spin probe in DMPC. Three charged peptides were studied: pentagastrin, an analogue with positions 4 and 5 reversed (i.e., ending in Phe-Asp-$NH_2$), and one with Asp replaced by Arg at position 4. All three of these charged peptides altered the phase transition behavior of DMPC to give two components, one above and one below the transition temperature of the pure lipid. With increasing peptide concentration, the higher melting transition became more prominent. The arginine-containing peptide produced the largest shifts in melting temperature followed by pentagastrin and then the "reversed" peptide. The arginine-containing peptide also increased the enthalpy of the transition. These peptides also increased the ordering of DMPC below the phase transition as measured with both 5- and 16-doxylstearic acid. The ordering effect was most pronounced with the arginine-containing peptide using the 5-doxylstearic acid probe. The results demonstrate that even the zwitterionic DMPC can interact more strongly with positively charged peptides than with negatively charged ones. In addition, peptide sequence as well as composition is important in determining the nature of peptide–lipid interactions. The markedly different effects of these pentagastrin peptides on the phase transition and motional properties of DMPC occur despite the similar depth of burial of these peptides with DMPC [see Surewicz, W. K., & Epand, R. M. (1984) *Biochemistry 23*, 6072–6077].

Studies of lipid–protein interactions in model systems provide basic information about the organization of biological membranes. It is well established that the phase transition characteristics of phospholipids as well as the bilayer order and fluidity can be affected in different ways by various proteins. The variety of effects observed in reconstituted systems are thought to reflect different types of lipid–protein interactions (Papahadjopoulos et al., 1975b; Boggs, 1983). The molecular basis of these effects and particularly the relationship between the mode of interaction and the chemical composition of lipid–protein systems are, however, not fully understood. Moreover, apart from elucidating the molecular nature of lipid–protein interactions in biomembranes, the understanding of the mode of association between lipids and peptides is of interest in view of the apparent relationship between this interaction and the potency of biologically important peptides in binding to specific receptor sites of biological membranes (Epand, 1983; Gysin & Schwyzer, 1983; Epand et al., 1985).

We have investigated these questions using a series of peptides related to pentagastrin. Pentagastrin is a chemically modified form of the carboxyl-terminal tetrapeptide of the hormone gastrin. It has potent biological activity, and a large number of structure–function studies have been done with this drug (Morley, 1968). In our initial study of these systems, we have compared the lipid binding properties of these peptides using fluorescence spectroscopy (Surewicz & Epand, 1984). The current study reports an investigation of the properties of dimyristoylphosphatidylcholine (DMPC)–pentapeptide complexes using high-sensitivity differential scanning calorimetry (DSC) and electron spin resonance (ESR) spin-labeling techniques. These two complementary methods provide a macroscopic description of the thermodynamic state of the membrane (DSC) and a microscopic description of the local ordering and fluidity of the phospholipid acyl chains (ESR). The peptides (all amino acids in the L configuration) used in the present work are *N*-*t*-Boc-β-Ala-Trp-Met-Asp-Phe-$NH_2$ (pentagastrin) (I), *N*-*t*-Boc-β-Ala-Trp-Met-Arg-Phe-$NH_2$ (II), *N*-*t*-Boc-β-Ala-Trp-Met-Gly-Phe-$NH_2$ (III), *N*-*t*-Boc-β-Ala-Trp-Met-Phe-Phe-$NH_2$ (IV), and *N*-*t*-Boc-β-Ala-Trp-Met-Phe-Asp-$NH_2$ (V). The above series of peptides allows for the systematic study of the effects of peptide structure on the mode of interaction between these peptides and phospholipids. The role of electrostatic charge, hydrophobicity, and amino acid sequence can be evaluated. It is shown that even relatively small changes in peptide structure may dramatically affect the mode of interaction of the peptide with phospholipids.

## Experimental Procedures

*Materials.* Dimyristoylphosphatidylcholine (DMPC) was purchased from Calbiochem and was purified by recrystalli-

† This work was supported by the Medical Research Council of Canada (Grant MT 7654).

‡ On leave from the Department of Biophysics, University of Lodz, Poland.

0006-2960/85/0424-3135$01.50/0 

zation from chloroform–hexane (Albon & Sturtevant, 1978). Pentagastrin (*N-t*-Boc-β-Ala-Trp-Met-Asp-Phe-$NH_2$), *N-t*-Boc-β-Ala-Trp-Met-Phe-Asp-$NH_2$, and *N-t*-Boc-β-Ala-Trp-Met-Arg-Phe-$NH_2$ were from Peninsula Labs. *N-t*-Boc-β-Ala-Trp-Met-Gly-Phe-$NH_2$ and *N-t*-Boc-β-Ala-Trp-Met-Phe-Phe-$NH_2$ were from Bachem, Inc. Each of the peptides was shown to be at least 95% pure by high-pressure liquid chromatography (HPLC) using a 15-cm Varian MCH-5, C-18 reverse-phase column with a gradient elution from 80% $H_2O$, 0.1% trifluoroacetic acid, and 20% 2-propanol to pure 2-propanol. Spin-labels, 5-doxylstearic acid and 16-doxylstearic acid, were from Molecular Probes, Inc.

*Sample Preparation.* Samples for differential scanning calorimetry experiments were prepared by two different procedures, depending on the water solubility of the peptides used. With two peptides of very limited water solubility (*N-t*-Boc-β-Ala-Trp-Met-Gly-Phe-$NH_2$ and *N-t*-Boc-β-Ala-Trp-Met-Phe-Phe-$NH_2$), the peptides were dissolved in chloroform–methanol (1:1), and the appropriate amount of this stock solution was mixed with 2 mg of lipid. The solvent was evaporated to dryness first under nitrogen and then in a vacuum dryer for 3–4 h. Two milliliters of standard PIPES buffer [20 mM piperazine-*N*,*N*′-bis(2-ethanesulfonic acid) (PIPES), 1 mM ethylenediaminetetraacetic acid (EDTA), and 150 mM NaCl, pH 7.4] was added to the peptide–lipid film, and the mixture was vortexed for approximately 10 min during which time the sample was warmed and cooled repeatedly through the transition temperature. In a few samples containing high peptide concentrations, the sample was also sonicated in a Branson bath-type sonicator for 30 s in order to facilitate the dispersion of the lipid–peptide mixture. We verified that such a very mild sonication does not affect the transition profile of these lipid–peptide complexes. The three more water-soluble peptides (*N-t*-Boc-β-Ala-Trp-Met-Asp-Phe-$NH_2$, *N-t*-Boc-β-Ala-Trp-Met-Phe-Asp-$NH_2$, and *N-t*-Boc-β-Ala-Trp-Met-Arg-Phe-$NH_2$) were dissolved in PIPES buffer, and samples were prepared by adding 2 mL of this solution to 1 mg of a dry lipid film, followed by vortexing as described above.

For the preparation of samples used for ESR measurements, appropriate amounts of lipid, spin-label, and peptide were dissolved in chloroform–methanol (1:1). After evaporation of the solvent, PIPES buffer was added, and the mixture was shaken by means of a vortex rotamixer as described above. The final DMPC concentration was 40 mg/mL. The spin-label:DMPC molar ratio was 1:100. Due to the high concentration of material required in the ESR experiments and the limited water solubility of all the peptides studied, in no case could samples be prepared from aqueous peptide solutions as employed in some cases for DSC.

It not stated otherwise, samples were incubated overnight at 8 °C before measurement. The low incubation temperature has been chosen in view of the previous observation that these pentapeptides incorporate into DMPC liposomes more readily below than above the phase transition temperature (Surewicz & Epand, 1984).

In all cases, peptide concentrations are given as the total peptide concentration in the system, including both the aqueous and lipid phases. In the case of the uncharged peptides, containing Gly or Phe at position 4, virtually all of the peptide must be in the membrane phase since these peptides are very sparcely soluble in water. In the cases of the other peptides, the partitioning is dependent on the temperature as well as on the concentration of lipid and peptide (Surewicz & Epand, 1984).

*Differential Scanning Calorimetry.* Calorimetric scans were performed with a high-sensitivity differential scanning calorimeter, MICROCAL-2 (Microcal, Inc., Amherst, MA). The scanning rate was usually 24 °C/h. The sample cell volume was 1.29 mL. A flat base line was observed with buffer in both sample and reference cells. The temperature of maximal excess heat capacity was defined as the phase transition temperature.

*ESR Measurements.* ESR spectra were obtained with a Bruker ER 100 D ESR spectrometer operating at 9.5 GHz. The spectrometer was equipped with a variable-temperature accessory.

ESR spectra of spin-labeled membranes were analyzed in terms of a polarity-corrected order parameter. The order parameter, $S$, is a measure of the amplitude of the motion of the molecular long axis about the average orientation of the fatty acid chains in the lipid bilayer. It is obtained from the anisotropic hyperfine splittings, $A_\parallel$ and $A_\perp$, by the equation (Hubbel & McConnell, 1971)

$$S = \frac{A_\parallel - A_\perp}{A_{xx} - \frac{1}{2}(A_{yy} + A_{zz})} \frac{a}{a'} \quad (1)$$

In this equation, $A_{xx}$, $A_{yy}$, and $A_{zz}$ are components of the hyperfine splitting tensor obtained from single-crystal spectra, $a = (A_{xx} + A_{yy} + A_{zz})/3$ and $a' = (A_\parallel + 2A_\perp)/3$. In some cases, $A_\parallel$ was also used as a measure of membrane order.

The motional parameter, $\tau$, of 16-doxylstearic acid labeled membranes above the phase transition temperature was measured from the expression (Keith et al., 1970)

$$\tau = (6.5 \times 10^{-10}) W_0[(h_0/h_{-1})^{1/2} - 1] \quad (2)$$

where $W_0$ is the width of the center line (in gauss), $h_0$ and $h_{-1}$ are the heights of the central and high-field lines, respectively, and the constant gives $\tau$ in units of seconds.

## Results

*Differential Scanning Calorimetry.* DSC scans of DMPC complexes with *N-t*-Boc-β-Ala-Trp-Met-Gly-Phe-$NH_2$ and *N-t*-Boc-β-Ala-Trp-Met-Phe-Phe-$NH_2$ are very similar. Some representative scans obtained with suspensions containing increasing amounts of *N-t*-Boc-β-Ala-Trp-Met-Gly-Phe-$NH_2$ are shown in Figure 1. Identical calorimetric traces were recorded after repeated scans of the samples. Also, preincubation of the suspensions for up to 24 h at different temperatures in the range of 8–40 °C did not affect the calorimetric profiles. It indicates that the DMPC–*N-t*-Boc-β-Ala-Trp-Met-Gly-Phe-$NH_2$ and DMPC–*N-t*-Boc-β-Ala-Trp-Met-Phe-Phe-$NH_2$ mixtures are at equilibrium. The effects of both peptides on the thermal behavior of DMPC exhibit several common features. First, the pretransition peak at approximately 14 °C disappears at relatively low peptide concentration (≥2 mol %). Second, the temperature of the main transition is virtually unaffected by the peptides. The most characteristic effect of both peptides on the phase transition profile of DMPC is a pronounced decrease in enthalpy change ($\Delta H$) associated with the transition (Figure 2). The decrease in $\Delta H$ is initially linear with respect to peptide concentration, and then it tends to saturate. Another common effect of *N-t*-Boc-β-Ala-Trp-Met-Gly-Phe-$NH_2$ and *N-t*-Boc-β-Ala-Trp-Met-Phe-Phe-$NH_2$ on the thermal behavior of DMPC is the broadening of the excess specific heat curves. This broadening is indicative of the decreased cooperativity of the transition, and it may be expressed in terms of the cooperative unit size ($k$) estimated from the relation (Mabrey & Sturtevant, 1978)

$$k = \Delta H_{VH}/\Delta H \quad (3)$$

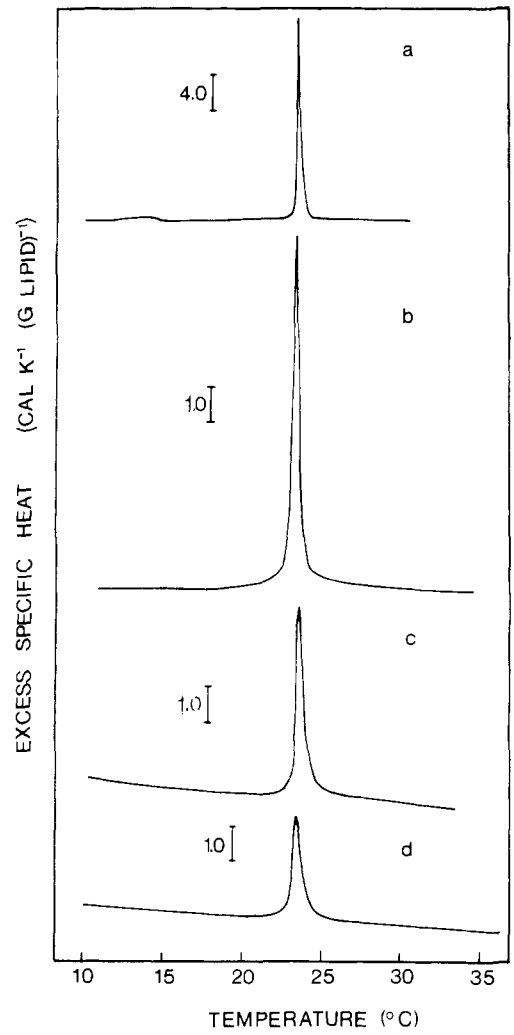


FIGURE 1: Representative DSC scans of DMPC–*N*-*t*-Boc-β-Ala-Trp-Met-Gly-Phe-$NH_2$ dispersions: (a) DMPC alone; (b) DMPC:peptide mole ratio of 10:1; (c) DMPC:peptide mole ratio of 5:1; (d) DMPC:peptide mole ratio of 1.25:1. Note that the curve for the pure lipid is drawn at a different scale than those for the lipid–peptide dispersions. The calibration mark for pure DMPC is the one given for 4 cal $K^{-1}$ (g of lipid)$^{-1}$ while the 1 cal $K^{-1}$ (g of lipid)$^{-1}$ calibration mark is given for the remaining curves.

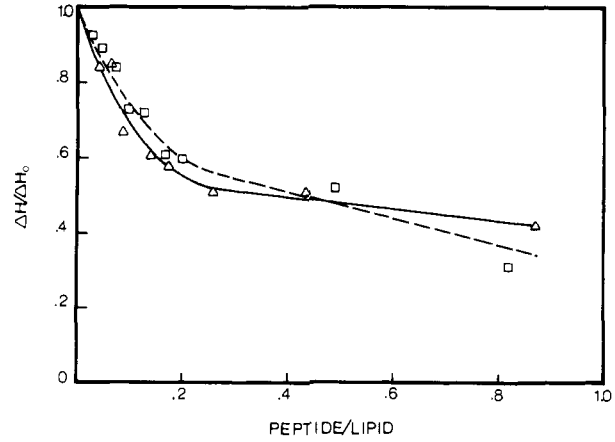


FIGURE 2: Effect of *N*-*t*-Boc-β-Ala-Trp-Met-Gly-Phe-$NH_2$ (□) and *N*-*t*-Boc-β-Ala-Trp-Met-Phe-Phe-$NH_2$ (△) on the enthalpy of the phase transition of DMPC dispersions. The enthalpies were obtained by integration of the calorimetric curves similar to those presented in Figure 1. $\Delta H_0$ is the enthalpy of the transition of pure lipid (5.2 kcal/mol), and $\Delta H$ is the enthalpy change associated with the transition of lipid–peptide dispersion. Peptide:lipid ratio represents the mole ratio of these two components.

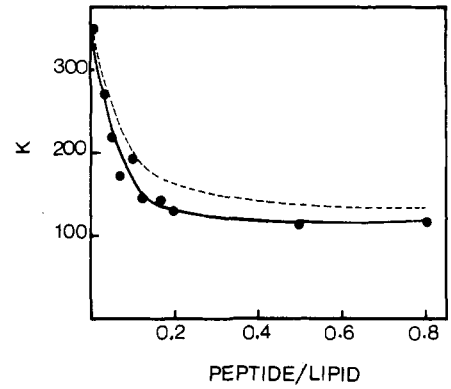


FIGURE 3: Effect of *N*-*t*-Boc-β-Ala-Trp-Met-Gly-Phe-$NH_2$ (●) and *N*-*t*-Boc-β-Ala-Trp-Met-Phe-Phe-$NH_2$ (---) on the cooperative unit size, *k*, of the phase transition of DMPC. For clarity of the figure, experimental points are omitted for the DMPC–*N*-*t*-Boc-β-Ala-Trp-Met-Phe-Phe-$NH_2$ system, and only the best-fit curve is shown. Peptide:lipid ratio represents the mole ratio of these two components.

where the van't Hoff enthalpy, $\Delta H_{VH}$, equals $4RT^2c_{max}/q$ ($R$, gas constant; $c_{max}$, maximum excess specific heat; $q$, area under the specific heat curve) and $\Delta H$ is the molar enthalpy associated with the transition of pure lipid. The value of $k$ obtained from eq 3 reflects the effective cooperative unit size of this fraction of DMPC molecules which still participates in the transition at a given lipid:peptide molar ratio (Correa-Freire et al., 1979). It is calculated with the assumption that, in the presence of peptides, a fraction of the lipid is removed from the transition but the molar enthalpy change of the remaining lipid fraction is the same as that of pure DMPC (see Discussion). As shown in Figure 3, there is a rapid 2–3-fold drop in the size of the cooperative unit at relatively low concentrations of the peptides, followed by a plateau region.

The thermotropic properties of DMPC complexes with the three less hydrophobic peptides are very different from those described above. Typical calorimetric scans of DMPC–pentagastrin mixtures are shown in Figure 4. Qualitatively, very similar scans were obtained in the presence of the "reversed" analogue of pentagastrin, *N*-*t*-Boc-β-Ala-Trp-Met-Phe-Asp-$NH_2$. With both peptides, the excess specific heat vs. temperature curves can be analyzed as a sum of two approximately symmetrical peaks: a relatively narrow low-temperature peak and a broader peak centered at higher temperature. As shown quantitatively in Figure 5, with increasing peptide concentration the two peaks become further separated. The narrow peak is shifted to lower temperatures with respect to the melting point of pure lipid whereas the broader peak moves toward higher temperatures. These effects are markedly more pronounced with pentagastrin than with its reversed analogue containing the Phe-Asp-$NH_2$ sequence. The shift in the temperature of the maximum excess specific heat of the two van't Hoff components is accompanied by their broadening, being particularly marked with the high-temperature peak. Again, the effect is more pronounced in the presence of pentagastrin than *N*-*t*-Boc-β-Ala-Trp-Met-Phe-Asp-$NH_2$ (data not shown). Similar results for pentagastrin–DMPC mixtures have been previously reported (Epand & Sturtevant, 1984). The splitting of the transition curves of DMPC into two components is observed also in the presence of low concentrations of *N*-*t*-Boc-β-Ala-Trp-Met-Arg-Phe-$NH_2$ (Figure 6). At higher concentrations of this peptide, however, the low-temperature peak disappeared, and only the high-temperature transition can be observed. Moreover, the upward shift of this transition with respect to the melting point of pure DMPC is much more dramatic than the effects observed with pentagastrin and its reversed analogue (Figure 5).

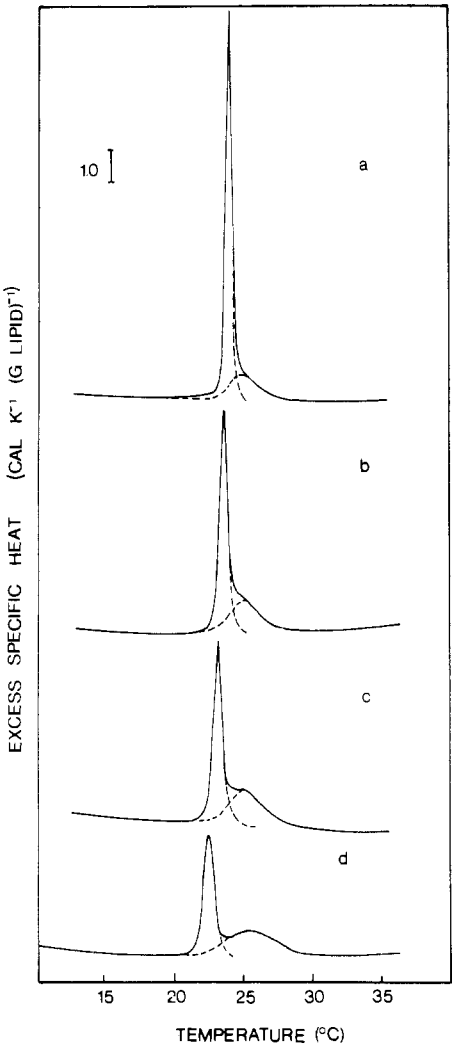


FIGURE 4: Representative DSC scans of DMPC dispersions (0.5 mg/mL) in the presence of different concentrations of pentagastrin (*N*-*t*-Boc-β-Ala-Trp-Met-Asp-Phe-$NH_2$): (a) 0.1 mM; (b) 0.2 mM; (c) 0.36 mM; (d) 0.65 mM. The dashed lines indicate the two components into which the transition curves have been resolved.

The total enthalpy of the transition of DMPC is not changed in the presence of pentagastrin and is slightly increased in the presence of *N*-*t*-Boc-β-Ala-Trp-Met-Phe-Asp-$NH_2$. On the other hand, *N*-*t*-Boc-β-Ala-Trp-Met-Arg-Phe-$NH_2$ produces a marked, concentration-dependent increase in the total enthalpy of the transition (Figure 7A). With all three peptides, at increased peptide concentration there is a gradual increase in the enthalpy of the higher temperature component at the expense of the lower temperature one (Figure 7B). This effect is particularly marked for *N*-*t*-Boc-β-Ala-Trp-Met-Arg-Phe-$NH_2$, in which case no low-temperature component can be seen above a peptide concentration of approximately 0.5 mM. Pentagastrin is here again more effective than its reversed analogue.

DSC scans of the DMPC–pentagastrin and the DMPC–*N*-*t*-Boc-β-Ala-Trp-Met-Phe-Asp-$NH_2$ complexes appear to be essentially insensitive to the temperature at which samples were preincubated before calorimetric measurements, and the repeated scans were identical with the original traces. In contrast, in the case of the DMPC–*N*-*t*-Boc-β-Ala-Trp-Met-Arg-Phe-$NH_2$ mixtures, the shape of the transition curve depends markedly on the thermal history of the sample. An example of this dependence is illustrated in Figure 8. A sample preincubated at 8 °C exhibits only one, high-temperature transition (upper scan in Figure 8). However, if this

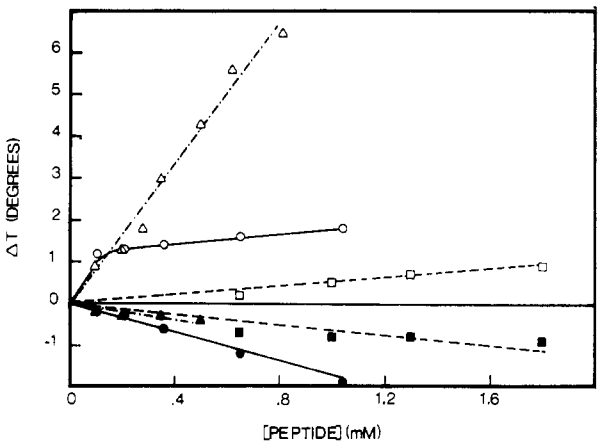


FIGURE 5: Change of the phase transition temperature of DMPC in the presence of pentagastrin (○, ●), *N*-*t*-Boc-β-Ala-Trp-Met-Phe-Asp-$NH_2$ (□, ■), and *N*-*t*-Boc-β-Ala-Trp-Met-Arg-Phe-$NH_2$ (△, ▲). The shifts in phase transition temperature were calculated with respect to the transition of pure DMPC (23.6 °C). The two transitions reported in the presence of the peptides were obtained by analyzing the observed transition curves into two van't Hoff components (cf. Figures 4 and 6). Open and closed symbols represent high-temperature and low-temperature transitions, respectively. Lipid concentration 0.5 mg/mL.

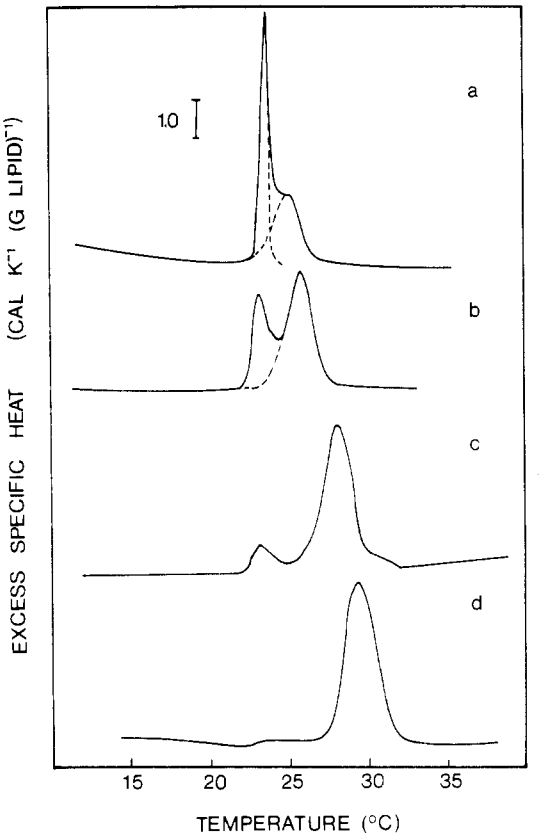


FIGURE 6: Representative DSC scans of DMPC dispersions (0.5 mg/mL) in the presence of different concentrations of *N*-*t*-Boc-β-Ala-Trp-Met-Arg-Phe-$NH_2$: (a) 0.2 mM; (b) 0.28 mM; (c) 0.5 mM; (d) 0.62 mM.

sample is rescanned without removing it from the calorimeter then a second, low-temperature transition appeared, and the enthalpy of the high-temperature transition was reduced (lower scan in Figure 8). This probably results from the partial dissociation of the complex above the phase transition temperature, as indicated by our previous fluorescence spectroscopy studies (Surewicz & Epand, 1984). As the lipid tends to aggregate in the calorimeter cell, especially during the slow

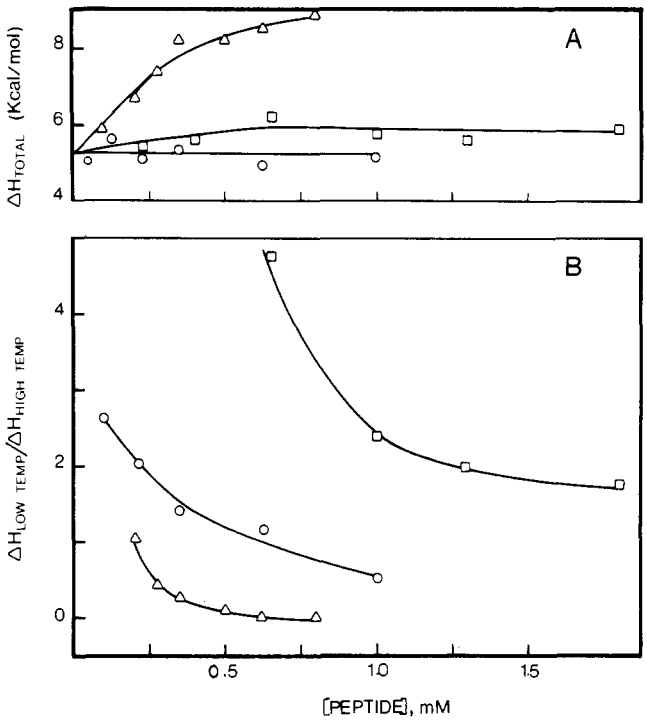


FIGURE 7: Effect of *N-t*-Boc-β-Ala-Trp-Met-Asp-Phe-$NH_2$ (○), *N-t*-Boc-β-Ala-Trp-Met-Phe-Asp-$NH_2$ (□), and *N-t*-Boc-β-Ala-Trp-Met-Arg-Phe-$NH_2$ (△) on the enthalpy of the DMPC phase transition. (A) Total enthalpy of the transition; (B) ratio of the calorimetric enthalpy of the low-temperature transition to that of the high-temperature transition of peptide mixtures with DMPC.

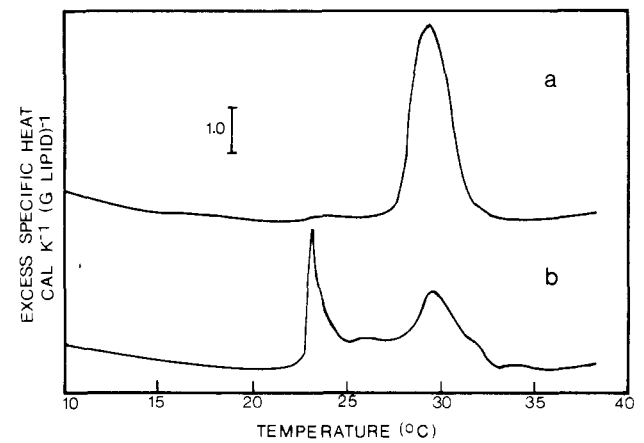


FIGURE 8: DSC thermograms of DMPC (0.5 mg/mL) in the presence of 0.62 mM *N-t*-Boc-β-Ala-Trp-Met-Arg-Phe-$NH_2$. (a) First scan of the sample preincubated overnight at 8 °C and loaded to a precooled calorimetric cell; (b) second scan of the same sample without withdrawing it from the calorimeter cell.

cooling of the calorimeter during thermal reequilibration, the rate of rebinding of this released peptide at low temperature may be severely hindered. Such an interpretation is supported by the observation that if the sample is withdrawn from the calorimeter after the first scan, remixed at a temperature below the phase transition, and reloaded into a precooled cell, then the low-temperature peak disappears again, and the DSC scan is virtually identical with the first scan shown in the upper part of Figure 8.

*Electron Spin Resonance.* 5-Doxylstearic acid monitors the motional properties of the bilayer region close to the lipid polar head group (Hubbel & McConnell, 1971; Schreier-Mucillo et al., 1976). The temperature dependence of the order parameter of 5-doxylstearic acid in DMPC multibilayers is shown in Figure 9. In accordance with previous studies (Hubbel &

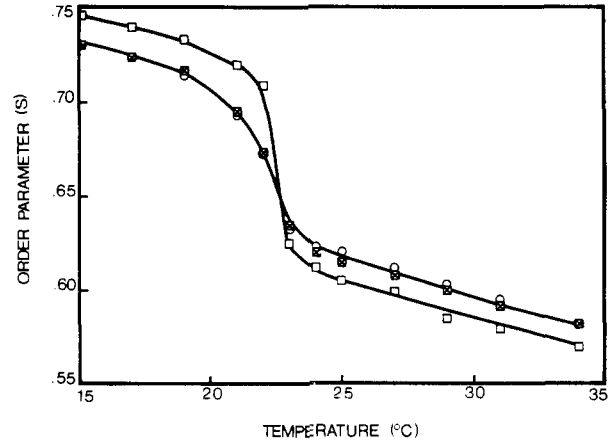


FIGURE 9: Temperature dependence of the order parameter, *S*, of 5-doxylstearic acid spin-label in DMPC alone (□) and DMPC complexed with 33 mol % *N-t*-Boc-β-Ala-Trp-Met-Gly-Phe-$NH_2$ (■) or with 33 mol % *N-t*-Boc-β-Ala-Trp-Met-Phe-Phe-$NH_2$ (○). Heating and cooling scans gave identical results.

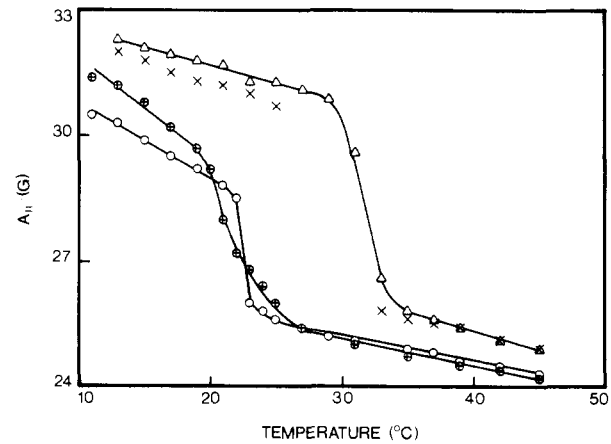


FIGURE 10: Temperature dependence of the $A_{||}$ parameter of 5-doxylstearic acid spin-label in DMPC alone (○) and DMPC complexed with 50 mol % pentagastrin (⊕) or with 35 mol % *N-t*-Boc-β-Ala-Trp-Met-Arg-Phe-$NH_2$. With this latter peptide, (△) represents the results of the heating scan, and (×) represents the results of the cooling scan. No data are given for the cooling scan in the temperature range where two components are present in the ESR spectra (cf. Figure 11). With DMPC alone and DMPC complexed with pentagastrin, cooling and heating scans were almost superimposable.

McConnell, 1971), there is a rapid drop in membrane order at the phase transition temperature. In the presence of either of the two relatively hydrophobic pentapeptides, *N-t*-Boc-β-Ala-Trp-Met-Gly-Phe-$NH_2$ and *N-t*-Boc-β-Ala-Trp-Met-Phe-Phe-$NH_2$, the temperature range of the ESR-detectable transition is broadened, the effect being compatible with the calorimetric data. Moreover, Figure 9 shows that these peptides produce some decrease in the molecular order of DMPC membranes below the transition temperature and increase the order of DMPC bilayers in the liquid-crystalline state.

The effects of other pentapeptides studied on the ESR spectra of 5-doxylstearic acid spin-labeled DMPC multibilayers differ significantly from those observed with *N-t*-Boc-β-Ala-Trp-Met-Phe-Phe-$NH_2$ and *N-t*-Boc-β-Ala-Trp-Met-Gly-Phe-$NH_2$. Figure 10 shows the temperature dependence of the spectral parameter $A_{||}$ of 5-doxylstearic acid in DMPC and DMPC complexed with pentagastrin and with *N-t*-Boc-β-Ala-Trp-Met-Arg-Phe-$NH_2$. $A_{||}$ instead of the order parameter *S* is plotted here against temperature as no inner hyperfine maximum could be resolved at low temperatures in the presence of the arginine-containing peptide. The data of the Figure 10 confirm the calorimetric observation of a marked

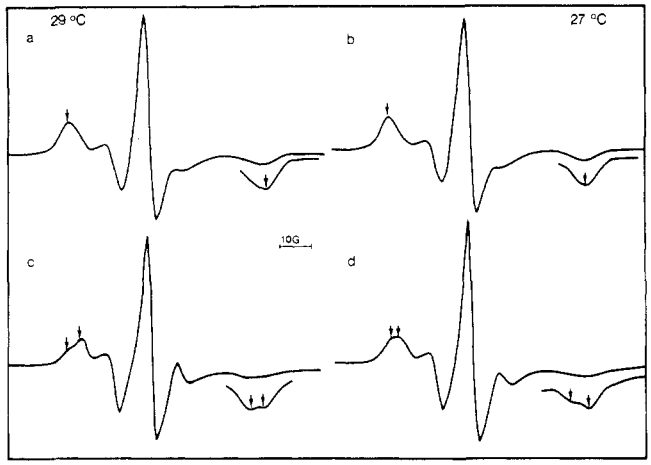


FIGURE 11: ESR spectra of 5-doxylstearic acid spin-label in DMPC complexed with 35 mol % *N*-*t*-Boc-β-Ala-Trp-Met-Arg-Phe-$NH_2$ at 27 (b and d) and 29 °C (a and c). The upper spectra at each temperature (a and b) represent the heating scan while the lower ones (c and d) were obtained with cooling scans. Note that two components are present in the cooling scan spectra.

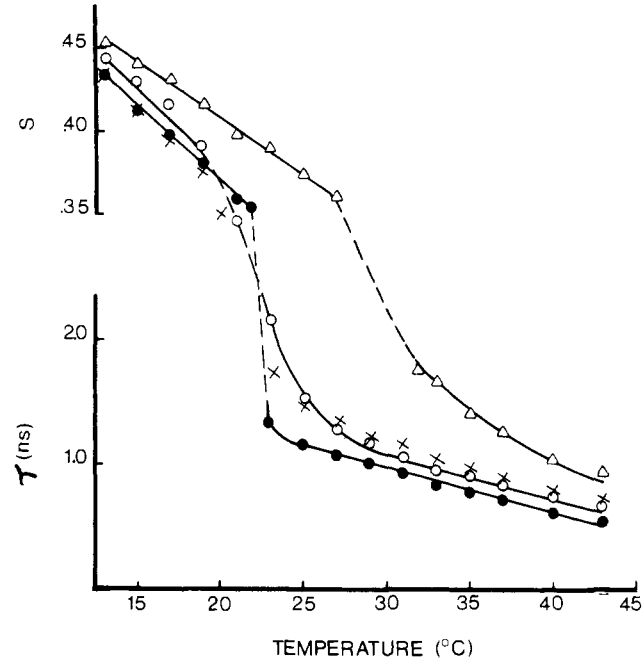


FIGURE 12: Temperature dependence of spectral parameters of 16-doxylstearic acid spin-label in DMPC (●) and DMPC complexed with 50 mol % pentagastrin (○), 35 mol % *N*-*t*-Boc-β-Ala-Trp-Met-Arg-Phe-$NH_2$ (△), or 33 mol % *N*-*t*-Boc-β-Ala-Trp-Met-Gly-Phe-$NH_2$ (×). $S$ is plotted at low temperatures, and $\tau$ is plotted at high temperatures. All plots represent heating scans. The presence of an immobilized component in the spectra of 16-doxylstearic acid may result in slight overestimation of $\tau$ values calculated according to eq 2. It is estimated that the resulting error does not exceed 5% of the reported $\tau$ values.

increase in the phase transition temperature of DMPC in the presence of *N*-*t*-Boc-β-Ala-Trp-Met-Arg-Phe-$NH_2$. Moreover, it is seen that this peptide produces a dramatic increase in the molecular order (as indicated by an increase in $A_\parallel$) of the gel-phase DMPC. The ordering effect of this peptide can also be observed above the phase transition temperature, although it is smaller and gradually diminishes as the temperature is increased. In view of the dependence of the DSC scans of DMPC–*N*-*t*-Boc-β-Ala-Trp-Met-Arg-Phe-$NH_2$ complexes on the thermal history of the sample (cf. Figure 8), the temperature dependence of $A_\parallel$ has been examined in both heating and cooling scans. In cooling from 30 to 25 °C, two components can be seen in the ESR spectra: one of the $A_\parallel$ values corresponding to that of the pure fluid lipid at the same temperature and one corresponding to a much more ordered lipid (Figure 11). No such splitting into two components is observed in the heating cycle after preincubation of the sample at 8 °C. The two components present in ESR spectra in the cooling scans are apparently related to the two transitions observed upon rescanning a sample by DSC (cf. lower scan in Figure 8). Both DSC and ESR data indicate that the partial dissociation of the lipid–peptide complex at higher temperature results in the phase separation of relatively ordered, peptide-rich domains and more fluid peptide-depleted domains.

With the DMPC–pentagastrin system, the $A_\parallel$ vs. temperature plots indicate a marked broadening of the phase transition (Figure 10). Apparently, the ESR technique fails to resolve two partially overlapping components present in the DSC scans. As with *N*-*t*-Boc-β-Ala-Trp-Met-Arg-Phe-$NH_2$, the molecular order of gel-state DMPC membranes is increased by pentagastrin, although in this case the effect is less pronounced. No significant change in $A_\parallel$ is produced by pentagastrin above the phase transition temperature of the lipid–peptide complex. The results of heating and cooling scans of this system are fully superimposable. The effects of *N*-*t*-Boc-β-Ala-Trp-Met-Phe-Asp-$NH_2$ on the $A_\parallel$ vs. temperature plots are qualitatively similar to those observed with pentagastrin although, in accordance with DSC data, the magnitude of these effects is significantly smaller (data not shown for brevity).

The 16-doxylstearic acid spin probe monitors the behavior of the relatively fluid inner hydrocarbon core of the lipid bilayer (Schreier-Mucillo et al., 1976). The ESR spectrum of this probe in DMPC membranes above the phase transition temperature is characteristic of fast, nearly isotropic motion, and it may be characterized by the motional parameter $\tau$ [for example, see Boggs & Moscarello (1978a)]. Below the phase transition temperature, the probe exhibits anisotropic motion which may be characterized by the order parameter. The effects of pentapeptides on the above spectral parameters of 16-doxylstearic acid labeled DMPC membranes are shown in Figure 12. *N*-*t*-Boc-β-Ala-Trp-Met-Arg-Phe-$NH_2$ produces a marked increase in both $\tau$ and $S$. Apparently, the ordering effect of this peptide on both gel and liquid-crystalline DMPC (cf. Figure 10) is not confined to the polar head group region of the bilayer only. The tendency to a more rigid disposition of the lipid moieties around the probe, caused by this peptide, exists also in the inner hydrophobic core of the bilayer. Some rigidification of the hydrophobic regions is observed also in the presence of pentagastrin. In this case, the effects are, however, very small. Two more hydrophobic pentapeptides, *N*-*t*-Boc-β-Ala-Trp-Met-Gly-Phe-$NH_2$ and *N*-*t*-Boc-β-Ala-Trp-Met-Phe-Phe-$NH_2$, have virtually no effect on the order parameter of 16-doxylstearic acid labeled membranes below the phase transition temperature. Above the transition temperature, these peptides produce some increase in $\tau$.

The interesting feature of 16-doxylstearic acid spin-labeled DMPC complexes with *N*-*t*-Boc-β-Ala-Trp-Met-Phe-Phe-$NH_2$, *N*-*t*-Boc-β-Ala-Trp-Met-Gly-Phe-$NH_2$, and pentagastrin, but not with *N*-*t*-Boc-β-Ala-Trp-Met-Arg-Phe-$NH_2$,[1] is that a second immobilized component can be distinguished

[1] It should be emphasized that the two components present in some ESR spectra of 5-doxylstearic acid labeled DMPC–*N*-*t*-Boc-β-Ala-Trp-Met-Arg-Phe-$NH_2$ samples are of an entirely different nature. In this latter case, two components are present only in the narrow temperature range between the phase transitions of two different membrane domains, and both of them show a strong dependence on temperature.

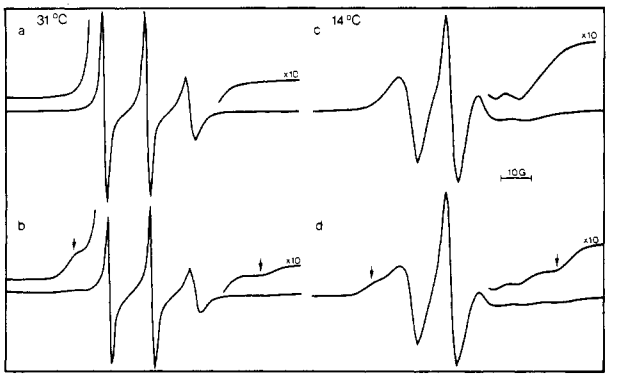


FIGURE 13: ESR spectra of 16-doxylstearic acid spin-label in DMPC and DMPC complexed with 33 mol % *N*-*t*-Boc-β-Ala-Trp-Met-Gly-Phe-$NH_2$: (a) DMPC at 31 °C; (b) DMPC–peptide mixture at 31 °C; (c) DMPC at 14 °C; (d) DMPC–peptide mixture at 14 °C. Arrows indicate the second immobilized component present in the spectra of DMPC–peptide samples. An identical immobilized component is present also in the ESR spectra of DMPC mixtures with *N*-*t*-Boc-β-Ala-Trp-Met-Phe-Phe-$NH_2$ and with pentagastrin.

in the ESR spectra (Figure 13). This immobilized component is present both below and above the phase transition temperature. The degree of immobilization of the spin-label fraction giving rise to this component appears to be independent of the physical state of bulk bilayer lipid, as the half distance between the outer hyperfine extrema is temperature independent, amounting to 37 G in a temperature range of 10–40 °C.

## Discussion

The data presented in this paper show that even relatively small changes in peptide structure resulting from substitution of a single amino acid may influence significantly the mode of peptide interaction with phospholipids.

*N*-*t*-Boc-β-Ala-Trp-Met-Gly-Phe-$NH_2$ and *N*-*t*-Boc-β-Ala-Trp-Met-Phe-Phe-$NH_2$, two peptides of very limited solubility in water, decrease the calorimetric transition enthalpy. This most likely indicates that in the presence of the peptides only a fraction of the total number of phospholipid molecules participates in the phase transition. According to this assumption, the linear portions of the enthalpy change vs. peptide concentration curves of Figure 2 may be conveniently analyzed in terms of the equation (Correa-Freire et al., 1979)

$$\frac{\Delta H}{\Delta H_0} = 1 - \langle n \rangle \frac{[\text{peptide}]}{[\text{lipid}]} \qquad (4)$$

where $\Delta H_0$ is the enthalpy change associated with the transition of pure lipid and $\langle n \rangle$ is the mean number of lipid molecules excluded from the transition per one peptide molecule. Such an analysis of the data indicates that at a peptide concentration of up to approximately 10–15 mol % (linear portions of the curves in Figure 2) one molecule of each peptide removes approximately two to three DMPC molecules from the cooperative gel to liquid-crystalline transition (the best-fit curves give values of 2.4 and 3.2 for *N*-*t*-Boc-β-Ala-Trp-Met-Gly-Phe-$NH_2$ and *N*-*t*-Boc-β-Ala-Trp-Met-Phe-Phe-$NH_2$, respectively).

The decrease in the enthalpy of the lipid phase transition, caused by *N*-*t*-Boc-β-Ala-Trp-Met-Gly-Phe-$NH_2$ and by *N*-*t*-Boc-β-Ala-Trp-Met-Phe-Phe-$NH_2$, is very similar to the effects observed at comparable protein to lipid weight ratios with integral membrane proteins (Papahadjopoulos et al., 1975a; Curatolo et al., 1977; Boggs & Moscarello, 1978b; Van Zoelen et al., 1978; Gomez-Fernandez et al., 1980, Freire et al., 1983) and hydrophobic polypeptides such as gramicidin A (Chapman et al., 1977). Two different mechanisms have been considered in the literature to account for the decrease in transition enthalpy of phospholipids in the presence of intrinsic membrane proteins. One involves the concept of an immobilized layer of "boundary" lipids which surround the protein and does not participate in the cooperative transition (Papahadjopoulos et al., 1975a; Curatolo et al., 1977; Boggs & Moscarello, 1978b; Freire et al., 1983). The alternative model proposed that below the transition temperature of phospholipids the system separates into domains of pure gel-phase lipid and protein clusters with entrapped lipids in a melted state (Chapman et al., 1977; Lookman et al., 1982; Davoust et al., 1980). Microcalorimetry cannot directly distinguish between these models. In view of the small size of the peptides, *N*-*t*-Boc-β-Ala-Trp-Met-Gly-Phe-$NH_2$ and *N*-*t*-Boc-β-Ala-Trp-Met-Phe-Phe-$NH_2$, the concept of a large lipid "annulus" is inappropriate. The marked negative deviations from linearity of $\Delta H/\Delta H_0$ vs. peptide:phospholipid mole ratio plots observed at higher peptide concentrations seem to indicate that the "entrapped lipid" model also may not be fully adequate for the description of the system considered, as the above model predicts a linear dependence if the entire melting process is taken into account (Lookman et al., 1982). The enthalpy change vs. peptide concentration plots of Figure 2 may perhaps be best explained by assuming that at low peptide concentrations randomly distributed lipid–peptide complexes are present whereas at higher concentrations the peptides tend to self-associate in the bilayer plane. Such a peptide self-association and/or formation of larger clusters would reduce the average number of peptide–lipid contacts.

With three other peptides studied, *N*-*t*-Boc-β-Ala-Trp-Met-Asp-Phe-$NH_2$, *N*-*t*-Boc-β-Ala-Trp-Met-Phe-Asp-$NH_2$, and *N*-*t*-Boc-β-Ala-Trp-Met-Arg-Phe-$NH_2$, the calorimetric curves can be resolved into two well-defined components (Figure 5). These transition components are not resolved in temperature plots of motional parameters of fatty acid spin-labels, indicating the ability of DSC to extract more detailed information in agreement with conclusions of other authors (McElhaney, 1984). Although the molecular basis for these complex calorimetric curves is not fully clear (Epand & Sturtevant, 1984), the two transition components very likely reflect the existence, at least in the gel state, of two distinct lipid regions in lipid–peptide mixtures (Bernard et al., 1982). If such an interpretation is correct, the high-temperature transition should be attributed to the melting of lipids belonging to peptide-rich domains while the remaining bulk lipid gives rise to the sharp low-temperature transition. The small downward shift and some broadening of the low-temperature transition compared with that of pure DMPC indicated, however, that the latter lipid fraction is also affected by the presence of peptide-rich domains. The above assignment of the transition components is strongly supported by the observation that with increasing peptide concentration there is a gradual increase in the enthalpies of the high-temperature components at the expense of the low-temperature ones. With the DMPC-*N*-*t*-Boc-β-Ala-Trp-Met-Arg-Phe-$NH_2$ system, the phase separation between high-temperature melting, peptide-rich regions, and low-temperature melting relatively unperturbed bulk lipid is evidenced also more directly by the ESR spectra of 5-doxylstearic acid labeled membranes in which two components are present in a temperature range between the two calorimetrically detectable transitions (cf. Figure 11).

The relative abilities of three water-soluble pentapeptides to perturb the thermotropic properties of DMPC membranes decrease in the order *N*-*t*-Boc-β-Ala-Trp-Met-Arg-Phe-$NH_2$

> *N*-*t*-Boc-β-Ala-Trp-Met-Asp-Phe-$NH_2$ > *N*-*t*-Boc-β-Ala-Trp-Met-Phe-Asp-$NH_2$. This coincides with the order of decreased lipid affinities of these peptides derived from fluorescence titration curves (Surewicz & Epand, 1984). In the presence of higher concentrations of *N*-*t*-Boc-β-Ala-Trp-Met-Arg-Phe-$NH_2$, the low-temperature transition disappears completely (Figure 6). Thus, in the case of this peptide, it is possible to have sufficient peptide present so that all of the lipid is transformed from the relatively unperturbed low-temperature melting state to a high-temperature melting, peptide-rich domain. This result demonstrates the greater effect of the arginine-containing peptide on the thermotropic properties of DMPC. Differences in the interaction of DMPC with anionic pentagastrin and with its cationic analogue *N*-*t*-Boc-β-Ala-Trp-Met-Arg-Phe-$NH_2$ manifest themselves not only in changes in the phase transition temperature but also in the transition enthalpy (Figure 7A). Mixtures of DMPC and *N*-*t*-Boc-β-Ala-Trp-Met-Arg-Phe-$NH_2$ exhibit a particularly large transition enthalpy. Increases in transition enthalpy are also observed on the binding of divalent metal ions to acidic phospholipids (Boggs & Rangaraj, 1983). Since the arginine-containing peptide binds more strongly to gel-state than to liquid-crystalline-state lipid (Surewicz & Epand, 1984), the dissociation of the peptide from the lipid near 24 °C may contribute to the observed transition enthalpy. This phenomenon is especially notable only for the cationic peptide *N*-*t*-Boc-β-Ala-Trp-Met-Arg-Phe-$NH_2$.

Multicomponent thermotropic transitions have often been observed with mixtures of lipids with proteins or peptides. However, in most cases the perturbed lipids show transitions at lower temperatures than that of the pure lipids (Papahadjopoulos et al., 1975b; Boggs & Moscarello, 1978a; Bernard et al., 1982; Sixl & Galla, 1982). According to a previous classification of lipid–protein interactions, the apperance of a high-temperature, high enthalpy transition was found only with negatively charged lipids exhibiting purely electrostatic surface absorption without penetration of the peptide into the bilayer (Papahadjopoulos et al., 1975b). These conditions are not fulfilled in our system, where the phospholipid is zwitterionic rather than acidic and the peptides can readily penetrate the bilayer, as indicated by a blue shift in the fluorescence spectra of the tryptophan residues (Surewicz & Epand, 1984). More recent studies indicated, however, that the pentapeptides studied here are not unique in their ability to induce the high-temperature transitions in synthetic phosphatidylcholine bilayers. Polymyxin B–DMPC has been shown by Raman spectroscopy to exhibit two transitions at approximately 26 and 38 °C, instead of a single transition at 23 °C of the pure phospholipid (Mushayakarara & Levin, 1984). Other polypeptides which solubilize phospholipids and contain sequences with hydrophobic amino acids regularly spaced at every third or fourth residue along the chain also raise the phase transition temperature of DMPC. These peptides and proteins include melittin at a certain concentration range (Levin et al., 1982; Prendergast et al., 1982), glucagon (Epand & Sturtevant, 1984), and apolipoprotein A (Jonas & Mason, 1981; Massey et al., 1981).

ESR studies with spin-labeled fatty acids can give information about order and motion in the bilayer, albeit in the presence of the nitroxide probe. *N*-*t*-Boc-β-Ala-Trp-Met-Gly-Phe-$NH_2$ and *N*-*t*-Boc-β-Ala-Trp-Met-Phe-Phe-$NH_2$ produce some decrease in the molecular order of 5-doxylstearic acid spin-labeled DMPC membranes in the gel state and increase the order of the bilayer in a liquid-crystalline state. The disordering effect of the peptides on the lipid bilayer below its $T_c$ is, in general, similar to what occurs with intrinsic membrane proteins and polypeptides such as gramicidin A (Curatolo et al., 1978; Gomez-Fernandez et al., 1980; Cortijo et al., 1982; Lee et al., 1984). The disordering effect of these pentagastrin analogues on the gel-state DMPC bilayer can be observed with the 5-doxylstearic acid spin-label but not with the 16-doxylstearic acid probe. Apparently, the peptides do not penetrate very deeply into the inner hydrophobic core of the membrane when lipids are in a gel state, or, alternatively, they adopt a conformation in which they can be accommodated in the bilayer without perturbing the organization near the center of the bilayer. Above the transition temperature, these peptides order the hydrophobic as well as the polar regions of the bilayer (Figures 9 and 12).

In contrast to *N*-*t*-Boc-β-Ala-Trp-Met-Gly-Phe-$NH_2$ and *N*-*t*-Boc-β-Ala-Trp-Met-Phe-Phe-$NH_2$, the peptides pentagastrin, *N*-*t*-Boc-β-Ala-Trp-Met-Arg-Phe-$NH_2$ and, to a smaller extent also, *N*-*t*-Boc-β-Ala-Trp-Met-Phe-Asp-$NH_2$ produce an increase in the order of the DMPC bilayer below the phase transition temperature. This ordering effect extends over the whole depth of the bilayer, although it is considerably stronger in the polar region. The relative potencies of these three pentapeptides to increase the order of the gel-state DMPC fully coincide with their abilities to increase the phase transition temperature of this phospholipid. The increase in order is particularly dramatic with *N*-*t*-Boc-β-Ala-Trp-Met-Arg-Phe-$NH_2$. The nature of the effect with this peptide is such, however, that it does not promote the appearance of a second immobilized component in the spectra. In addition, the observed ordering effect with this peptide is still present, albeit smaller, above the phase transition temperature of DMPC. This is in contrast to pentagastrin and *N*-*t*-Boc-β-Ala-Trp-Met-Phe-Asp-$NH_2$, which have very little effect on the liquid-crystalline-state DMPC.

Peptide-induced ordering of the gel-phase lipids is not a very common phenomenon, as a majority of proteins and peptides, both intrinsic and peripheral, exert an opposite effect. The pentapeptides studied here are, however, not unique in their ability to increase the molecular order of gel-state phospholipids (Epand et al., 1977; Boggs & Moscarello, 1978a; Boggs, 1983; Wiener et al., 1983). We believe that the pentapeptide-induced concomitant increases in the phase transition temperature and in the molecular order of the phospholipids far below the transition temperature are interrelated phenomena, and both of them reflect strong interaction of the peptide with gel-state lipids (Surewicz & Epand, 1984).

At higher concentrations of some of the pentapeptides studied, a second immobilized component has been observed in the ESR spectra of 16-doxylstearic acid labeled membranes (Figure 13). Similar immobilized components have been reported in the presence of various intrinsic membrane proteins and polypeptides. They have been considered by some authors as the evidence of a "boundary" layer of lipids surrounding the protein (Jost et al., 1973; Boggs & Moscarello, 1978b; Marsh et al., 1978). This interpretation has been recently criticized by Pink et al. (1984) on the basis of theoretical considerations and results of experiments employing other techniques than ESR. These authors conclude that although a fraction of the spin probe is strongly immobilized in the presence of integral membrane proteins, there is no evidence that unlabeled lipids experience similar immobilization. If this conclusion is correct, then our present ESR results with pentapeptides may suffer from the same ambiguity as a result of the use of probes. Further spectroscopic studies using unperturbing techniques such as NMR or IR spectroscopy are

required before any satisfactory explanation of the nature of the immobilized component in the ESR spectra of the spin-labeled DMPC–pentapeptide systems can be proposed. Nonetheless, the observation that the immobilized component is induced by the peptides, having dramatically different effects on the enthalpy of the lipid phase transition (cf. pentagastrin vs. uncharged, more hydrophobic analogues), strongly supports the conclusion (Gomez-Fernandes et al., 1980) that the fraction of lipid lacking a calorimetric transition cannot be equated with that fraction giving rise to an immobilized component in the ESR spectra.

In conclusion, the mode of peptide interaction with DMPC appears to be very sensitive to small changes in peptide structure. Electrical charge, hydrophobicity, and the relative sequence of amino acids are among the critical factors controlling peptide interaction with phospholipids. Replacement of negative charged aspartic acid, present at the fourth position in pentagastrin, with positively charged arginine results in a marked increase in the effects of the peptide on the properties of the lipid. This illustrates the importance of electrostatic interactions and the fact that certain cationic peptides can interact strongly even with zwitterionic lipids. On the other hand, the reversal of the order of the last two amino acids in pentagastrin produces marked weakening of the interaction, illustrating the importance of amino acid sequence and possibly amphiphatic structures (Surewicz & Epand, 1984). Pentapeptides containing the neutral amino acids glycine or phenylalanine at the fourth position interact differently with DMPC. These two relatively hydrophobic pentapeptides mimic many aspects of the effects produced in lipid bilayers by intrinsic membrane proteins and polypeptides.

This present work illustrates the marked differences that are exhibited in the interaction of a series of structurally related pentapeptides with phospholipids. These differences occur despite the fact that on the basis of our fluorescence studies (Surewicz & Epand, 1984) all of these pentagastrin-related peptides penetrate the DMPC bilayer to similar extents. Thus, the molecular basis for the observed differences in the interaction of these peptides with phospholipids is not simply due to differences in their ability to embed in the bilayer but rather to more specific factors. The different modes of the interaction of various pentagastrin analogues with DMPC could reflect different extents of peptide self-association in the bilayer plane. Such an association is particularly likely below the phase transition temperature of phospholipids and at high peptide concentrations (Uemura et al., 1983; Epand & Surewicz, 1984). We do not believe, however, that this is a major factor giving rise to the differences in the properties of the various peptides since the effects of the peptides are present even when they are in low concentration in the membrane and the effects increase progressively with larger peptide to lipid ratios. Other factors include electrostatic interactions, even with the zwitterionic lipid DMPC. This interaction may be particularly strong between the arginine side chain of the peptide and the phosphate group of DMPC. The mode of peptide–lipid interaction may also be controlled to some extent by the conformational properties of the pentapeptides. These are likely to be affected even by a small change in the amino acid composition of the peptides.

**Registry No.** I, 5534-95-2; II, 92762-75-9; III, 92762-76-0; IV, 96194-48-8; V, 92762-74-8; DMPC, 13699-48-4.

## REFERENCES


Albon, N., & Sturtevant, J. M. (1978) *Proc. Natl. Acad. Sci. U.S.A. 75*, 2258–2260.

Bernard, E., Faucon, J.-F., & Dufourcq, J. (1982) *Biochim. Biophys. Acta 688*, 152–162.

Boggs, J. M. (1983) in *Membrane Fluidity in Biology* (Aloia, R. C., Ed.) Vol. 2, pp 83–130, Academic Press, New York.

Boggs, J. M., & Moscarello, M. A. (1978a) *J. Membr. Biol. 39*, 75–96.

Boggs, J. M., & Moscarello, M. A. (1978b) *Biochemistry 17*, 5734–5739.

Boggs, J. M., & Rangaraj, G. (1983) *Biochemistry 22*, 5425–5435.

Chapman, D., Cornell, B. A., Eliasz, A. W., & Perry, A. (1977) *J. Mol. Biol. 113*, 517–538.

Correa-Freire, M. C., Freire, E., Barenholz, Y., Biltonen, R. L., & Thompson, T. E. (1979) *Biochemistry 18*, 442–445.

Cortijo, M., Alonso, A., Gomez-Fernandez, J. C., & Chapman, D. (1982) *J. Mol. Biol. 157*, 597–618.

Curatolo, W., Sakura, J. D., Small, D. M., & Shipley, G. (1977) *Biochemistry 16*, 2313–2319.

Curatolo, W., Verma, S. P., Sakura, J. D., Small, D. M., Shipley, G. G., & Wallach, D. F. H. (1978) *Biochemistry 17*, 1802–1807.

Davoust, J., Bienvenue, A., Fellmann, P., & Devaux, P. F. (1980) *Biochim. Biophys. Acta 596*, 28–42.

Epand, R. M. (1983) *Mol. Cell. Biochem. 57*, 41–47.

Epand, R. M., & Sturtevant, J. M. (1984) *Biophys. Chem. 19*, 355–362.

Epand, R. M., & Surewicz, W. K. (1984) *Can. J. Biochem. Cell Biol. 62*, 1167–1173.

Epand, R. M., Jones, A. J. S., & Sayer, B. (1977) *Biochemistry 16*, 4360–4368.

Epand, R. M., Epand, R. F., & Orlowski, R. C. (1985) *Int. J. Pept. Protein Res. 25*, 105–111.

Freire, E., Markello, T., Rigell, C., & Holloway, P. W. (1983) *Biochemistry 22*, 1675–1680.

Gomez-Fernandez, J. C., Goni, F. M., Bach, D., Restall, C. J., & Chapman, D. (1980) *Biochim. Biophys. Acta 598*, 502–516.

Gysin, B., & Schwyzer, R. (1983) *FEBS Lett. 158*, 12–16.

Hubbel, W. L., & McConnell, H. M. (1971) *J. Am. Chem. Soc. 93*, 314–326.

Jonas, A., & Mason, W. R. (1981) *Biochemistry 20*, 4603–4606.

Jost, P. C., Griffith, O. H., Capaldi, R. A., & Vanderkooi, G. (1973) *Proc. Natl. Acad. Sci. U.S.A. 70*, 480–484.

Keith, A. D., Bulfield, G., & Snipes, W. (1970) *Biophys. J. 10*, 618–623.

Lee, D., Durrani, A. A., & Chapman, D. (1984) *Biochim. Biophys. Acta 769*, 49–56.

Levin, I. W., Lavialle, F., & Mollay, C. (1982) *Biophys. J. 37*, 339–349.

Lookman, T., Pink, D., Grundke, E. W., Zuckermann, M. J., & de Verteuil, F. (1982) *Biochemistry 21*, 5593–5601.

Mabrey, S., & Sturtevant, J. (1978) *Methods Membr. Biol. 9*, 237–274.

Marsh, D., Watts, A., Mesche, W., & Knowles, P. F. (1978) *Biochem. Biophys. Res. Commun. 81*, 397–402.

Massey, J. B., Gotto, A. M., & Pownall, H. J. (1981) *Biochemistry 20*, 1575–1584.

McElhaney, R. N. (1984) *Biochim. Biophys. Acta 779*, 1–42.

Morley, J. S. (1968) *Proc. R. Soc. London, B 170*, 97–111.

Mushayakarara, E., & Levin, I. W. (1984) *Biochim. Biophys. Acta 769*, 585–595.
Papahadjopoulos, D., Vail, W. J., & Moscarello, M. A. (1975a) *J. Membr. Biol. 22*, 143–164.
Papahadjopoulos, D., Moscarello, M. A., Eylar, E. H., & Isac, T. (1975b) *Biochim. Biophys. Acta 401*, 317–335.
Pink, D. A., Chapman, D., Laidlaw, D. J., & Wiedmer, T. (1984) *Biochemistry 23*, 4051–4058.
Prendergast, F. G., Lu, J., Wei, G. J., & Bloomfield, V. A. (1982) *Biochemistry 21*, 6963–6971.
Schreier-Mucillo, S., Marsh, D., & Smith, I. C. P. (1976) *Arch. Biochem. Biophys. 172*, 1–11.
Sixl, F., & Galla, H.-J. (1982) *Biochim. Biophys. Acta 693*, 466–478.
Surewicz, W. K., & Epand, R. M. (1984) *Biochemistry 23*, 6072–6077.
Uemura, A., Kimura, S., & Imanishi, Y. (1983) *Biochim. Biophys. Acta 729*, 28–34.
Van Zoelen, E. J. J., Van Dijck, P. W. M., De Kruijff, B., Verkleij, A. J., & Van Deenen, L. L. M. (1978) *Biochim. Biophys. Acta 514*, 9–24.
Wiener, J. R., Pal, R., Barenholz, Y., & Wagner, R. R. (1983) *Biochemistry 22*, 2162–2170.

# Solvent Isotope Effects for Lipoprotein Lipase Catalyzed Hydrolysis of Water-Soluble *p*-Nitrophenyl Esters†

Daniel M. Quinn
*Department of Chemistry, The University of Iowa, Iowa City, Iowa 52242*
*Received November 5, 1984*

ABSTRACT: Solvent deuterium isotope effects on the rates of lipoprotein lipase (LpL) catalyzed hydrolysis of the water-soluble esters *p*-nitrophenyl acetate (PNPA) and *p*-nitrophenyl butyrate (PNPB) have been measured and fall in the range 1.5–2.2. The isotope effects are independent of substrate concentration, LpL stability, and reaction temperature and hence are effects on chemical catalysis and not due to a medium effect of $D_2O$ on LpL stability and/or conformation. pL (L = H or D) vs. rate profiles for the $V_{max}/K_m$ of LpL-catalyzed hydrolysis of PNPB increase sigmoidally with increasing pL. Least-squares analysis of the profiles gives $pK_a^{H_2O} = 7.10 \pm 0.01$, $pK_a^{D_2O} = 7.795 \pm 0.007$, and a solvent isotope effect on limiting velocity at high pL of $1.97 \pm 0.03$. Because the pL–rate profiles are for the $V_{max}/K_m$ of hydrolysis of a water-soluble substrate, the measured $pK_a$'s are intrinsic acid–base ionization constants for a catalytically involved LpL active-site amino acid side chain. Benzeneboronic acid, a potent inhibitor of LpL-catalyzed hydrolysis of triacylglycerols [Vainio, P., Virtanen, J. A., & Kinnunen, P. K. J. (1982) *Biochim. Biophys. Acta 711*, 386–390], inhibits LpL-catalyzed hydrolysis of PNPB, with $K_i = 6.9$ μM at pH 7.36, 25 °C. This result and the solvent isotope effects for LpL-catalyzed hydrolysis of water-soluble esters are interpreted in terms of a proton transfer mechanism that is similar in many respects to that of the serine proteases.

Lipoprotein lipase (LpL)[1] plays a central role in cardiovascular lipid metabolism [see Quinn et al. (1983) for a review]. Its primary physiological task is the hydrolytic cleavage of the *sn*-1 and *sn*-3 ester bonds of triacylglycerols that are transported in the bloodstream in VLDL and chylomicrons. The catabolic products of LpL catalysis, IDL and chylomicron remnants, are thought if cholesteryl ester rich to be particularly atherogenic (Zilversmit, 1977, 1979). Lack of plasma LpL activity (Havel & Gordon, 1960) or of the LpL activator apoC-II (Breckenridge et al., 1978; Cox et al., 1978) is correlated with clinical manifestations of serum hypertriacylglycerolemia. It has been suggested that chylomicron and VLDL surface elements that are released from the catabolic lipolysis complex are nascent HDL (Tall & Small, 1980). The case for an antiatherogenic role for HDL appears to be gaining momentum with the passage of time (Kannel et al., 1979; Miller, 1980).

Despite the great physiological significance of LpL activity, there are glaring inadequacies in our knowledge of the enzyme's catalysis. This dearth of information obtains from the fact that the details of the chemical steps of LpL action have not been defined, which in turn hampers efforts to build a thoroughgoing biodynamical model of such molecular events as activation of LpL by interaction with lipid interfaces (Shirai & Jackson, 1982) or with apoC-II [see Quinn et al. (1983) and references cited therein]. Furthermore, efforts to design synthetic effectors of LpL catalysis, whether they be inhibitors or activators, cannot proceed until chemical catalysis by the enzyme is understood.

This paper represents the initiation of efforts to expose the chemical strategies employed by LpL to achieve its catalytic aim. Solvent deuterium isotope effects for the LpL-catalyzed hydrolysis of the water-soluble substrates *p*-nitrophenyl acetate (PNPA) and *p*-nitrophenyl butyrate (PNPB) have been measured and delineated as specific effects on the rates of chemical steps of catalysis, rather than as effects of $D_2O$ on

† This work was supported by U.S. Public Health Service New Investigator Research Award HL-30089.

[1] Abbreviations: LpL, lipoprotein lipase; IDL, intermediate-density lipoproteins; HDL, high-density lipoproteins; VLDL, very low density lipoproteins; PNPA, *p*-nitrophenyl acetate; PNPB, *p*-nitrophenyl butyrate; $V_i$, initial velocity; $V_{max}$, maximal velocity; $K_m$, Michaelis constant; apoC-II, apolipoprotein C-II; PMSF, phenylmethanesulfonyl fluoride; $K_i$, competitive inhibitor dissociation constant; pL, pH or pD; PNP, *p*-nitrophenoxide; Tris, tris(hydroxymethyl)aminomethane.

0006-2960/85/0424-3144$01.50/0 